Potential radiation-pressure-induced instabilities in cavity interferometers

Brian Meers and Norman MacDonald
Department of Physics and Astronomy, University of Glasgow, Glasgow G12 8QQ, Scotland
(Received 18 April 1989)

The mirrors of an interferometer may be rendered dynamically unstable by the radiation pressure of the sensing light. We assess the importance of this effect for optical cavities, concentrating in particular on proposed laser-interferometric gravitational wave detectors. Both broadband and narrow-band systems are considered. While the potential instabilities may well be important for cavities with weak suspensions, realistic gravitational wave detectors should not encounter any problems.

INTRODUCTION

Many different types of interferometer use Fabry-Pérot cavities to enhance a signal. A motion of the mirrors of such a cavity produces not only a phase change on the light emerging from it, but also an intensity change inside the cavity. The resultant change in radiation pressure will act back on the mirrors. This paper will address the question of whether the feedback due to the radiation pressure will be of sufficient magnitude to render the cavity unstable to small perturbations. In particular, we will investigate the importance of such effects for long baseline interferometric gravitational wave detectors.[1]

That radiation pressure changes in a Fabry-Pérot cavity might be dynamically significant is not a new idea. Braginsky and Manukin[2] pointed out that the radiation pressure in a cavity that is not perfectly resonant will have two effects: it will provide a "rigidity" or spring action which either acts against or reinforces any perturbation, depending on which side of resonance the cavity is operating; and the changing radiation pressure provides a damping or antidamping, again depending on the operating point. If the spring action is to stabilize, the "damping" will tend to destabilize (the phase delay due to the storage time of the cavity tends to destabilize the radiation-pressure feedback system). Instability will result if this dominates the effect of the mirror suspension. The spring action of the radiation pressure has been experimentally observed by Dorsel *et al.*[3] and discussed by Meystre *et al.*[4]

Independently, Tourrenc and co-workers have considered the effect on stability of a non-negligible cavity storage time. This was first emphasized by Deruelle and Tourrenc,[5] with linear destabilization in the presence of a phase offset being indicated by Aguirregabiria and Bel.[6] Subsequent papers described an approximate differential-equation treatment[7] and a numerical investigation of mirror motion in the unstable regime.[8] These results have been reviewed by Tourrenc and Aguirregabiria.[9] In some of these papers the possible danger of delay-induced instability in interferometric gravitational wave detectors is stressed.

We aim here to clear up any uncertainty concerning the stability of realistic gravitational wave detectors. In order to do this we include the effects of a possible servo system which acts to position and maintain the mirrors at the correct operating point on the cavity resonance curve (effectively raising the natural angular frequency Ω_0 of the mirror suspension as well as providing damping). We also provide analyses of the problem in both time and frequency domains, with no restriction on possible time delays. The time domain analysis extends the work of Ref. 6 using a stability boundary method, while the frequency domain analysis is easily applicable to the realistic cases where recycling is used in both broadband and narrow-band mode[10–12] and leads to simple expressions for the power required for the onset of instability in the cases. It will be seen that raising the frequency Ω_0 and lowering the quality factor Q of the mirror resonance dramatically increases the critical power. While the discussion will concentrate on interferometric gravitational wave detectors, a similar analysis is applicable to other cavity interferometers.

RADIATION PRESSURE IN THE FREQUENCY DOMAIN

In order to determine the dynamical consequences of radiation pressure changes we will consider a small perturbation, at angular frequency ω, to the position of one of the test masses of an interferometer and calculate the resulting change in intensity and in radiation pressure in the detector cavities. This may be expressed as frequency-dependent spring and damping terms which, combined with corresponding terms due to the mirror suspension (or servo system), give an effective oscillator differential equation. The stability conditions can then be found.

There are several possible optical arrangements to be considered. We will restrict ourselves to a simple cavity Michelson interferometer (see Fig. 1, without mirrors M_0, and M_3), or to the same system with either standard, detuned or dual recycling.[10–12] All these variants may be analyzed with the same mathematical method.

First consider a laser beam, initial amplitude E_0, incident on a cavity with mirrors of amplitude reflection

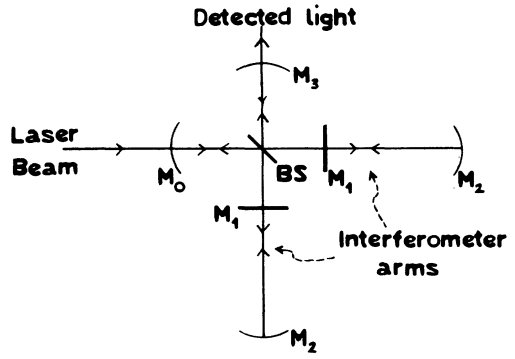

FIG. 1. Optical arrangement of a cavity gravitational wave detector. The Michelson interferometer operates with output port on a dark fringe. Standard recycling places mirror M_0 to recycle the laser power. Dual recycling adds M_3 to recycle signal sidebands.

coefficients R_1 and R_2 and transmission T_1 and T_2. Following the traditional treatment of a Fabry-Pérot cavity,[13] we may regard the field E_c inside the cavity as being the sum of many beams, each of which has experienced a different number of reflections inside the cavity:

$$E_c/E_0 = T_1 R_2 \sum_{N=1}^{\infty} (R_1 R_2)^{N-1} e^{iN\delta} , \tag{1}$$

where δ is the static phase offset from resonance. So

$$E_c/E_0 = \frac{T_1 R_2}{(1-R_1 R_2)^2} \left[\frac{e^{i\delta} - R_1 R_2}{1 + F' \sin^2 \delta/2} \right] , \tag{2}$$

where

$$F' = \frac{4F^2}{\pi^2} = \frac{4R_1 R_2}{(1-R_1 R_2)^2} .$$

F is the finesse of the cavity.

Now consider a perturbation $x = x_0 \cos(\omega t)$ to the length of the cavity. For the general case to be considered here, it is convenient to use an explicit sideband representation, in which the length change x is regarded as phase modulating the light in the cavity to produce two sidebands:

$$\delta\phi = \frac{2\pi}{\lambda} x_0 (e^{i\omega t} + e^{-i\omega t}) , \tag{3}$$

where $\delta\phi$ is the phase shift and λ is the wavelength of the light. The field is multiplied by $e^{i\delta\phi} \approx 1 + i\delta\phi$. Thus sideband fields at frequencies offset by $\pm\omega$ from the laser light are produced by each beam in the cavity. The total sideband field is obtained by adding up these contributions. The signal from the interferometer is contained in the sideband fields.

At this point the differences between the different optical arrangements should be considered. For a simple cavity system (no recycling), both laser light and sidebands have the same reflectivity off the cavity mirrors. In standard and detuned recycling, the sideband reflectivity is just determined by the properties of M_1 and M_2, but the effective reflectivity of the input mirror for the laser frequency is determined by both M_0 and M_1 (together with their separation); in other words, the input mirror in recycling may be viewed as being made up of the cavity formed by M_0 and M_1. The sidebands do not see this cavity as they exit via the beamsplitter output port. In dual recycling, however, the sidebands are reflected back in by M_3. The input mirror for the sidebands must then be viewed as consisting of the cavity formed by M_3 and M_1. To express, this, we will regard the input mirror as having reflectivity R_{1c} for the carrier and R_{1+} and R_{1-} for the $+\omega$ and $-\omega$ sidebands, respectively. If R_1 is defined to be real, then there is an associated phase change β on reflection from this "mirror." This may be absorbed into the phase offset δ which will therefore, in general, be different for the three frequencies of interest: δ_c, δ_+, and δ_-.

We can now add up the sideband fields generated on each bounce. Consider just the $+\omega$ field E_+ in the cavity:

$$\frac{E_+}{E_0} = -T_{1c} R_2^2 \frac{2\pi}{\lambda} x_0 e^{i\omega t} \times \sum_{N=1}^{\infty} (R_{1c} R_2)^{N-1} e^{iN\delta_c} \times \sum_{N=1}^{\infty} (R_{1+} R_2)^{N-1} e^{in\delta_+} e^{-in\omega/v_0} , \tag{4}$$

where $v_0 = c/2l$ is the free spectral range of the cavity, of length l. The $e^{-in\omega/v_0}$ term expresses the change in phase of the signal over the history of the light which is stored in the cavity. So

$$\frac{E_+}{E_0} = i \frac{2\pi}{\lambda} x_0 e^{i\omega t} \frac{T_{1c} R_2^2 e^{i(\delta_c + \delta_+ - \omega/v_0)}}{(1 - R_{1c} R_2 e^{i\delta_c})(1 - R_{1+} R_2 e^{i(\delta_+ - \omega/v_0)})} , \tag{5}$$

or

$$\frac{E_+}{E_0} = \frac{i 2\pi x_0 e^{i\omega t} T_{1c} R_2^2 (e^{i\delta_c} - R_{1c} R_2)(e^{i(\delta_+ - \omega/v_0)} - R_{1+} R_2)}{\lambda (1 - R_{1c} R_2)^2 (1 - R_{1+} R_2)^2 (1 + F_c' \sin^2 \delta_c/2)\{1 + F'_+ \sin^2[(\delta_+ - \omega/v_0)/2]\}} , \tag{6}$$

where

$$F_c' = \frac{4R_{1c} R_2}{(1 - R_{1c} R_2)^2} , \quad F'_+ = \frac{4R_{1+} R_2}{(1 - R_{1+} R_2)^2} .$$

For the other sideband, $+\omega \rightarrow -\omega$.

This basic expression can be used to derive either the gravitational wave signal or the intensity change in the cavity. Note that both detuned and dual recycling work

by making $\delta_c=0$ and $\delta_+=\omega/\nu_0$ (or $\delta_-=-\omega/\nu_0$) to maximize the sideband amplitude. Henceforth we will assume that M_2 is highly reflecting and set $R_2=1$ when it appears as a multiplier (but keeping $1-R_2=\frac{1}{2}A^2$).

The intensity change inside the cavity is

$$\delta I_c=(E_c+E_++E_-)(E_c^*+E_+^*+E^*)\ , \tag{7}$$

where E^* is the complete conjugate of E. The fluctuating parts of the intensity are, to first order,

$$\delta I_c=E_cE_+^*+E_c^*E_++E_cE_-^*+E_c^*E_-\ . \tag{8}$$

Just taking the $+\omega$ sideband for the moment, this gives

$$\frac{\delta I_{c+}}{I_0}=\frac{\left[\frac{T_{1c}}{1-R_{1c}R_2}\right]^2\frac{2\pi}{\lambda}x_0 i[e^{i\omega t}(e^{i(\delta_+-\omega/\nu_0)}-R_{1+}R_2)-e^{-i\omega t}(e^{-i(\delta_+-\omega/\nu_0)}-R_{1+}R_2)]}{(1-R_{1+}R_2)^2\left[1+F_c'\sin^2\left[\frac{\delta_c}{2}\right]\right]\left[1+F_+'\sin^2\frac{\delta_+-\omega/\nu_0}{2}\right]} \tag{9}$$

or

$$\frac{\delta I_{c+}}{I_0}=\frac{T_{1c}^2 2\pi x_0[-R_{1+}R_2\sin(\omega t)+\sin(\omega t+\delta_+-\omega/\nu_0)]}{\lambda(1-R_{1c}R_2)^2(1-R_{1+}R_2)^2[1+F_c'\sin^2(\delta_c/2)]\{1+F_+'\sin^2[(\delta_+-\omega/\nu_0)/2]\}}\ , \tag{10}$$

where I_0 is the laser power incident on the detector. This may be rewritten as ($\delta\ll 1$)

$$\frac{\delta I_{c+}}{I_0}=\frac{2\pi x_0 T_{1c}^2\{\cos[\omega t(\delta_+-\omega/\nu_0)]+\sin[\omega t(1-R_{1+}R_2)]\}}{\lambda(1-R_{1c}R_2)^2(1-R_{1+}R_2)^2[1+F_c'\sin^2(\delta_c/2)]\{1+F_+'\sin^2[(\delta_+-\omega/\nu_0)/2]\}}\ . \tag{11}$$

Adding the effect of the two sidebands then gives the total intensity fluctuation in the cavity:

$$\begin{aligned}\frac{\delta I_c}{I_0}=&\frac{2\pi x_0 T_{1c}^2}{\lambda(1-R_{1c}R_2)^2[1+F_c'\sin^2(\delta_c/2)]}\\&\times\left[\cos(\omega t)\left[\frac{(\delta_+-\omega/\nu_0)F_+^2/\pi^2}{1+F_+'\sin^2[(\delta_+-\omega/\nu_0)/2]}+\frac{(\delta_-+\omega/\nu_0)F_-^2/\pi^2}{1+F_-'\sin^2[(\delta_-+\omega/\nu_0)/2]}\right]\right.\\&\left.+\sin(\omega t)\left[\frac{F_+/\pi}{1+F_+'\sin^2[(\delta_+-\omega/\nu_0)/2]}-\frac{F_-/\pi}{1+F_-'\sin^2[(\delta_-+\omega/\nu_0)/2]}\right]\right]\ .\end{aligned} \tag{12}$$

SIMPLE INTERFEROMETERS

The general expression (12) applies to any of the optical arrangements. Consider first an interferometer with no recycling. In this case $\delta_c=\delta_+=\delta_-$ and $R_{1c}=R_{1+}=R_{1-}$. The intensity change in the cavity can then be written as

$$\begin{aligned}\frac{\delta I_c}{I_0}=&\frac{2\pi x_0 T_1^2F^2/\pi^2}{\lambda(1-R_1R_2)[1+F'\sin^2(\delta/2)]}\\&\times\left[\cos(\omega t)\left[\frac{(F/\pi)(\delta-\omega/\nu_0)}{1+F'\sin^2[(\delta-\omega/\nu_0)/2]}+\frac{(F/\pi)(\delta+\omega/\nu_0)}{1+F'\sin^2[(\delta+\omega/\nu_0)2]}\right]\right.\\&\left.+\sin(\omega t)\left[\frac{1}{1+F'\sin^2[(\delta-\omega/\nu_0)/2]}-\frac{1}{1+F'\sin^2[(\delta+\omega/\nu_0/2]}\right]\right]\end{aligned} \tag{13}$$

or

$$\frac{\delta I_c}{I_0}=\frac{4\pi x_0 T_1^2(F/\pi)^3\delta\{\cos(\omega t)[1+(F/\pi)^2(\delta^2-\omega^2/\nu_0^2)]+(2F\omega/\pi\nu_0)\sin(\omega t)\}}{\lambda(1-R_1R_2)[1+F'\sin^2(\delta/2)]\{1+F'\sin^2[(\delta+\omega/\nu_0)/2]\}\{1+F'\sin^2[(\delta-\omega/\nu_0)/2]\}}\ . \tag{14}$$

This expression contains some rather interesting features. As expected, the intensity in the cavity only changes (to first-order) if the cavity is not perfectly resonant ($\delta\neq 0$). For small offsets ($F\delta/\pi\ll 1$), the intensity change is proportional to δ; it is opposite for offsets on opposite sides of the fringe. Also, at very high frequency $F\omega/\pi\nu_0\gg 1$ the intensity changes are very small:

$$\left|\frac{\delta I_c}{I_0}\right| \propto \left[\frac{F\omega}{\pi\nu_0}\right]^{-2} = (\omega\tau_s)^{-2} \quad \text{if } \delta \ll \omega/\nu_0 , \tag{15}$$

where $\tau_s = 2Fl/\pi c$ is the storage time, the $1/e$ decay time for the cavity field. Both of these features arise because phase modulation (the original perturbation) is only converted into amplitude modulation if the two sidebands resonate *differently* in the cavity. Even if the laser frequency is well down the cavity resonance curve the two sidebands resonate similarly (and poorly) if they are offset by a frequency that is large compared with the cavity linewidth.

The radiation-pressure force contains components that are of the same (or opposite) phase and of the quadrature phase to the original motion. The in-phase component acts like a spring, the quadrature component provides damping or antidamping. Note that the quadrature term is proportional to minus the velocity, so when the spring is stable, antidamping is produced which tends to destabilize the system. In the low storage time case $F\omega/\pi\nu_0 \ll 1$, the damping increases with increasing storage time (or "delay"). However, the magnitude of the antidamping falls for high $\omega\tau_s$.

How does the radiation pressure affect the dynamics of the cavity? The expression for the changing intensity may be converted into a differential equation for changes in cavity length ($m\ddot{x} = 2\delta I_c/c$, m is the reduced mass of both mirrors):

$$\ddot{x} - \frac{2\tau_s\Omega_r^2}{1+(F^2/\pi^2)(\delta^2-\omega^2/\nu_0^2)}\dot{x}\Omega_r^2 x = 0 , \tag{16}$$

where

$$\Omega_r^2 = \frac{8\pi I_0 T_1^2 (F/\pi)^3 \delta[1+(F^2/\pi^2)(\delta^2-\omega^2/\nu_0^2)]}{\lambda mc(1-R_1R_2)[1+F'\sin^2(\delta/2)]\{1+F\sin^2[(\delta+\omega/\nu_0)/2]\}\{1+F'\sin^2[(\delta-\omega\nu_0)/2]\}} , \tag{17}$$

where we have taken the case of the "spring" term being stable, producing an antidamped resonance at Ω_r. If the mirror position is maintained by a damped spring of angular frequency Ω_0 and quality factor Q_0 (either mechanically or via an appropriate servo system), the equation governing the cavity length becomes

$$\ddot{x} + \dot{x}\left[\frac{\Omega_0}{Q_0} - \frac{2\tau_s\Omega_r^2}{1+(F^2/\pi^2)(\delta^2-\omega^2/\nu_0^2)}\right] + (\Omega_r^2+\Omega_0^2 x) = 0 . \tag{18}$$

This system will be unstable if

$$\frac{2\tau_s\Omega_r^2}{1+(F^2/\pi^2)(\delta^2-\Omega^2/\nu_0^2)} > \frac{\Omega_0}{Q_0} , \tag{19}$$

where Ω is the new natural frequency:

$$\Omega^2 = \Omega_0^2 + \Omega_r^2 . \tag{20}$$

Combining (19) and (20) we find an expression for the frequency Ω_i at which any instability will occur:

$$\Omega_i^2 = \frac{\Omega_0^2 + \frac{\Omega_0}{2\tau_s Q_0}\left[1+\frac{F^2\delta^2}{\pi^2}\right]}{1+\frac{\Omega_0\tau_s}{2Q_0}} . \tag{21}$$

This general expression is a little messy, though useful for numerical work. In any practical situation, however, we may assume an offset from resonance that is small $F\delta/\pi \ll 1$ ($F\delta/\pi$ is the fractional offset on the fringe). Further simplification is obtained if we restrict attention to the two limiting cases: of a resonance either with very little damping ($Q_0 \gg 1$) or with damping close to critical ($Q_0 \approx 1/2$). (It must be emphasized that a low Q does not necessarily give poor thermal noise performance, since the sensor may have a low noise temperature: the noise performance of an interferometer is not altered by the presence of a wideband, well-damped servo system. The signal remains as the force required to keep the test masses stationary relative to the light.) If $Q_0 \gg 1$, then reference to (21) shows that $\Omega_i^2 \approx \Omega_0^2$, i.e., the instability frequency will lie close to the oscillator-servo frequency.

On the other hand, if $Q_0 \approx \frac{1}{2}$, we find the simple result

$$\Omega_i^2 \approx \frac{\Omega_0^2}{\Omega_0\tau_s} = \Omega_0/\tau_s \tag{22}$$

or

$$(\Omega_i\tau_s)^2 = \Omega_0\tau_s . \tag{23}$$

So high damping requires a significant change in natural frequency for instability—the radiation-pressure feedback system must dominate the artificial servo. Knowing the eigenfrequency, we can substitute back into (19), using (17), to find an expression for the incident power I_0 required for instability. Remembering that the offset is small ($F\delta/\pi \ll 1$, $\delta < \omega/\nu_0$), then the high-Q_0 case gives

$$I_0 > \frac{\Omega_0[1+(\Omega_0\tau_s)^2]^2\lambda m l^2}{8\pi Q_0 c\tau_s^3(F\delta/\pi)} , \tag{24}$$

while the low-Q case ($Q_0 \approx \frac{1}{2}$) gives

$$I_0 > \frac{\Omega_0(1+\Omega_0\tau_s)^2\lambda m l^2}{8\pi Q_0 c\tau_s^3(F\delta/\pi)} . \tag{25}$$

Note that (25) is valid for all Q values in the sense that if the inequality is not satisfied, the system will be stable. A simple cavity interferometer is guaranteed to be stable as long as the power is less than I_{crit}:

$$I_{\text{crit}} = 6\times 10^{6}[\Omega_0(10^3\ \text{rad}\,s^{-1})](Q_0)^{-1} \times[m(100\ \text{kg})][l(3\ \text{km})]^2[\tau_s(\text{ms})]^{-3} \times(10^2F\delta/\pi)^{-1}\ \text{W} . \quad (26)$$

The parameters chosen here are quite conservative for a gravitational wave detector; for example, the servo on the University of Glasgow 10-m prototype has $\Omega_0 \approx 10^4$ rad s^{-1} and $Q_0 \approx 1$. λ is assumed to be 0.5 μm.

So very high power levels are required to obtain instability in such a system. If, however, we were to choose a system with $\Omega_0 = 6$ rad s^{-1}, $Q \sim 10^8$, $l = 10$ m, $m = 10$ kg, $F\delta/\pi = 1$, and $\tau_s = 300\mu s$, instability might be observed at a power level of only $\sim 10^{-10}$ W. Small systems with weak suspensions and little damping are more susceptible to radiation-pressure-induced instabilities.

RECYCLED INTERFEROMETERS

Realistic gravitational wave detectors will use recycling. Standard recycling increases the power circulating round the interferometer , so reducing the laser power required for the onset of stability. This can be incorporated by choosing $\delta_c = 0$ (maximum power enhancement) and a value of T_{1c} compatible with the degree of recycling. If the losses in the detector cavities dominate any losses at the beamsplitter, maximum power build up is obtained by choosing $T_{1c}^2 = 2A^2$, where A^2 is the loss coefficient ($R^2 + T^2 + A^2 = 1$), assumed to be equal in both cavity mirrors. Rewriting (12) then gives the intensity change in a detector cavity:

$$\frac{\delta I_c}{I_0} = \frac{2\pi x_0(F/\pi)^2\delta\{\cos(\omega t)[1+(F^2/\pi^2)(\delta^2-\omega^2/\nu_0^2)]+(2F\omega/\pi\nu_0)\sin(\omega t)\}}{\lambda A^2\{1+F'\sin[(\delta+\omega/\nu_0)/2]\}\{1+F'\sin^2[(\delta-\omega/\nu_0)/2]\}} , \quad (27)$$

where F is the finesse of the detector cavities. This is larger than the simple case by a factor $\pi/4FA^2$ for low loss cavities. Reference to (25) then indicates that an interferometer with standard recycling will be stable as long as

$$I_0 < \frac{\Omega_0(1+\Omega_0\tau_s)^2\lambda m l A^2}{4\pi Q_0\tau_s^2(F\delta/\pi)} . \quad (28)$$

Or, more simply and more stringently, stability will be ensured in standard recycling as long as

$$I_0 < 10^5[\Omega_0(10^3\ \text{rad}\,s^{-1})][m(100\ \text{kg})](Q_0)^{-1} \times[l(3\ \text{km})][\tau_s(\text{ms})]^{-2}(10^4A^2)(10^2F\delta/\pi)^{-1}\ \text{W} . \quad (29)$$

Current designs do not imagine more than 200 W being used. So a large broadband interferometer with a reasonable servo system should not encounter any problems with radiation-pressure-induced instabilities.

Both detuned and dual recycling may be used to enhance a signal within a restricted bandwidth. We wish to determine the stability properties of such systems.

In the usual way of operating dual recycling, and in detuned recycling, $\delta_+ = \delta_-$ and $F_+ = F_-$ to high accuracy. Other cases will not be discussed here, The expression (27) for the intensity change in standard recycling may then be used, with the understanding that F is the finesse that the signal sees, i.e., the detector cavity finesse in detuned recycling and the finesse determined by M_3 and M_1 in dual recycling. Thus, when operated in a broadband mode, dual and detuned recycling have the same stability properties as a standard recycling system with the same signal storage time.

When operated in narrow-band mode, the signal finesse is made high and the optical system tuned to make either of the two signal sidebands perfectly resonant. Now a single, perfectly resonant sideband provides pure damping or antidamping, since the intensity change lags the phase change by 90° [cf. (11) with $\delta_+ = \omega/\nu_0$]. If worried about radiation-pressure-induced instabilities, it would therefore seem sensible to choose to resonate the sideband which damps any motion. The only concern then is whether the spring action will push the cavity off its proper operating point to produce a zero-frequency instability. This would require $\Omega_r^2 > \Omega_0^2$ at $\omega = 0$, which, when the detector is tuned to a frequency ν_g, needs a power

$$I_0 > 2\Omega_0^2A^2\lambda m l\nu_g . \quad (30)$$

Or, stability is assured if the laser power is less than

$$I_{\text{crit}} = 3\times 10^3[\Omega_0(10^3\ \text{rad}\,s^{-1})]^2[m/(100\ \text{kg})] \times[l(3\ \text{km})][\nu_g(100\ \text{Hz})](10^4A^2)\ \text{W} . \quad (31)$$

Again, the interferometer should be stable at reasonable power levels.

It is interesting to see how the critical power for a narrow-band system alters if the other sideband is resonated. The detector will tend to go unstable at $\Omega_i \approx \omega_g$, the frequency of maximum antidamping, with a critical power

$$I_{\text{crit}} = \frac{4\pi\Omega_0\lambda mc\nu_g(A^2)^2}{Q_0} \quad (32)$$

or

$$I_{\text{crit}} = 200[\Omega_0(10^3\ \text{rad}\,\text{s}^{-1})] \times[\nu_g(100\ \text{Hz})][m(100\ \text{kg})](10^4A^2)^2\ \text{W} . \quad (33)$$

This is significantly lower critical power than the other sideband.

While the discussion of narrow-band systems has been confined to detuned and dual recycling, similar results should apply to resonant recycling: all of the narrow-band arrangements share the same characteristic of ensuring perfect resonance for both the laser light and one sideband. In addition, a delay line system that uses dual recycling will have the same stability properties as a corresponding cavity system.

CHARACTERISTIC EQUATION

In this section we consider the connections between the results so far and the treatment of the simple cavity by Aguirregabiria and Bel.[6] They treat the dynamics of a suspended mirror with delayed radiation pressure by linearization about a fixed point. Their linearized equation of motion contains an infinite series of delayed restoring force terms. Any one of these, if treated by a Taylor-series expansion in the delay, suffices to make the differential equation of infinite order.[14] Consequently, the characteristic equation has an infinite number of roots. However, those significant for the onset of instability are the pure imaginary roots, corresponding to a complex conjugate pair of roots moving from one half plane to the other. The characteristic equation with pure imaginary root $z=i\beta$ has at most two roots in the range of delays that are relevant. This equation gives two real equations, of the form

$$\beta^2-\Omega_0^2=F(\alpha,\beta)\ , \tag{34}$$

$$\frac{\beta\Omega_0}{Q_0}=G(\alpha,\beta)\ , \tag{35}$$

to be solved for the eigenfrequency β and a bifurcation parameter α. This process resembles that in the effective force treatment above, in which a damping force term is set equal to zero and the restoring force term in then used to give the frequency Ω_i.

Our previous method regarded the noise as consisting of a set of Fourier components, the effects of which were analyzed largely in the frequency domain. In contrast, the method of the characteristic equation studies the time evolution of an initial offset. However, we do not expect the linear stability of a system to depend on either the form of the perturbation or the domain of analysis. Indeed, we shall see that the two approaches do give the same answer for the stability of a simple cavity interferometer.

When the cavity length l, or the corresponding passage time $2l/c=1/\nu_0$ is taken as the bifurcation parameter, at constant power I_0, and fixed values of the optical parameters, there is either no instability, for low enough I_0, or else there is instability over a finite intermediate range of cavity length. We can interpret this in terms of the location of the sidebands on the resonance peak. By treating the mean delay as fixed, and the reflectivity as the bifurcation parameter (or the cavity length, since these are now not independent parameters) and by looking at the case of almost perfect reflectivity, we obtain an expression for the eigenfrequency β that is independent of I_0 and of the reflectivity. This turns out to be identical to Eq. (21), once we make clear the distinction between the mean delay used here and the storage time used so far.

The linearized delay-differential equation of Aguirregabiria and Bel[6] is

$$\frac{d^2x(t)}{dt^2}+\frac{\Omega_0}{Q_0}\frac{dx(t)}{dt}+\Omega_0^2x(t) = -A\sum_{k=0}^{\infty}\cos^k\theta\sin(k\delta)(t-k/\nu_0)\ . \tag{36}$$

Here we change their notation to conform with that adopted in the rest of this paper. They take the suspended mirror M_2 to be perfectly reflecting, and the mirror M_1 to have $R^2=\cos^2\theta$, $T^2=\sin^2\theta$. We shall follow their practice of parametrizing the phase offset δ as $\delta=\frac{1}{2}\gamma\theta^2$, where $0<\gamma<1$. So $\gamma=F\delta/\pi$ in the notation used earlier. (In their paper δ is denoted ε, γ is denoted δ, and ν_0^{-1} is denoted r.) The constant A is

$$A=\frac{16\pi I_0}{Mc\lambda}\Delta\sin^2\theta\ , \tag{37}$$

with

$$\Delta=(1+\cos^2\theta-2\cos\theta\cos\delta)^{-1}\ . \tag{38}$$

The characteristic equation corresponding to Eq. (36) is

$$z^2+\frac{z\Omega_0}{Q_0}+\Omega_0^2=-A\sum_k\cos^k\theta\sin(k\delta)e^{-zk/\nu_0} \tag{39}$$

or, for pure imaginary eigenvalue $z=i\beta$,

$$\beta^2-\Omega_0^2-\frac{i\beta\Omega_0}{Q_0}=A\sum_k\cos^k\theta\sin(k\delta)e^{-i\beta k/\nu_0}\ . \tag{40}$$

The Fourier series can be summed explicitly, and the result is conveniently expressed to contain a delay-dependent factor $H(i\phi)=H(i\beta/\nu_0)$. This factor tends to 1 for zero delay ($\nu_0\to\infty$), is real, negative, and very small for $\beta/\nu_0=\pi$, and is periodic with period 2π. Equation (40) becomes

$$\beta^2-\Omega_0^2-\frac{i\beta\Omega_0}{Q_0}=A\Delta(\cos\theta)(\sin\delta)H(i\phi)\ , \tag{41}$$

with

$$H(i\phi)=\frac{1+\cos^2\theta-2(\cos\theta)(\cos\delta)}{e^{i\phi}+e^{-i\phi}\cos^2\theta-2(\cos\theta)(\cos\delta)}\ . \tag{42}$$

We first take ν_0 as bifurcation parameter. The qualitative nature of the problem is illustrated in the schematic diagram, Fig. 2. The parabola is traced out as β increases from zero. The closed curve is traced out as ϕ increases from 0 to 2π. At low I_0 there are no intersections, and so no pure imaginary root of (39) and no change from stability. For larger I_0 there are a pair of intersections (β_1,ϕ_1) and (β_2,ϕ_2). That with larger β has smaller ϕ and so larger ν_0. This gives destabilization as the cavity length increases, a pair of roots passing from the left-hand half-plane to the right-hand half plane. We show in the Appendix that the intersection corresponding to longer cavity length has the same pair of roots passing back into the

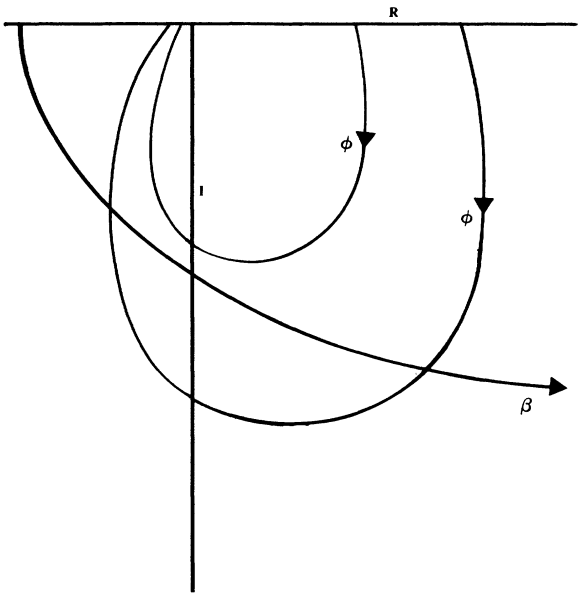

FIG. 2. Schematic diagram illustrating the possibility of restabilization. The parabola is traced out by the real and imaginary parts of the left-hand side of Eq. (38) as the eigenfrequency β increases. The other curves are two cases of the delay curve, traced out by the real and imaginary parts of the right-hand side of this equation as the parameter $\phi=\beta r=\beta/\nu_0$ increases from 0 to π. Since the parabola lies in the lower half plane the rest of the closed delay curve is not needed. The smaller of these curves is for low I_0; here no intersection means stability at any r. The larger is for high I_0; here there are two intersections.

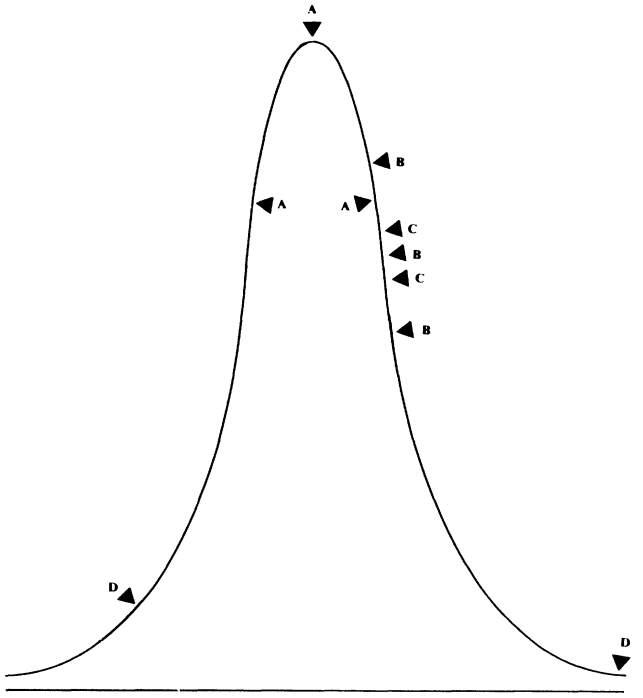

FIG. 3. Interpretation of restabilization in terms of the position on the resonance curve of the main beam and the sidebands. In the case *A*, with the main beam at the peak, there is no instability wherever we locate the symmetrically disposed sidebands. We suppose the case *B* to correspond to instability. Then one can return to stability either by moving the sidebands in to positions *C*, or out onto the shoulders of the peak at positions *D*.

left-hand half plane, giving restabilization.

That there is restabilization may also be seen by rewriting Eq. (25) in terms of the cavity length l,

$$I_{\text{crit}}=\frac{\Omega_0[1+\Omega_0(2Fl/\pi c)]^2\pi^2\lambda Mc^2}{64Q_0lF^3(F\delta/\pi)} . \tag{43}$$

Thus the power needed for instability has a minimum at about $2Fl\Omega_0/\pi c=1$.

Figure 3 shows how this may be interpreted in terms of sidebands. The frequency modulation is only translated into destabilizing intensity modulation if the two sidebands resonate differently. Thus if $\delta=0$ there can be no instability, since the sidebands are symmetrically arranged on the cavity resonance curve [Fig. 3(a)]. If $F\delta/\pi\cong 1$ and $\omega/\nu_0\ll\delta$, the laser light and the sidebands lie on the steep part of the curve [Fig. 3(b)]. The sidebands then resonate with different amplitude and phase, producing an intensity change which, for large enough I_0, will lead to instability. This destabilizing tendency is reduced if the cavity linewidth is made larger, by reducing l [Fig. 3(c)]. On the other hand, if $\omega/\nu_0\gg\delta$ the sidebands lie on the flat parts of the curve [Fig. 3(d)] and are of similar phase and (low) amplitude. One way to achieve this is to increase the length l.

We now take the mean delay T as fixed. From Eq. (36) an appropriate definition of mean delay is

$$\begin{aligned} T&=\sum_k\cos^k\theta\sin(k\delta)k/\nu_0\Big/\sum_k\cos^k\theta\sin(k\delta)\\ &=\frac{d}{dz}\ln H(z/\nu_0)\Big|_{z=0}\\ &=\frac{(1-\cos^2\theta)\nu_0^{-1}}{1+\cos^2\theta-2(\cos\theta)(\cos\delta)} . \end{aligned} \tag{44}$$

Thus $T\approx T_0=\mu\nu_0^{-1}\theta^{-2}$, with $\mu=4/(1+\gamma^2)$, to order θ^4. The conventional storage time τ_s used earlier is related to this by

$$\tau_s=2T_0/\mu . \tag{45}$$

We can now take either ν_0 or θ as the bifurcation parameter α, since they are not independent parameters in this case. The function H is no longer periodic, and has to be recomputed for each value of β. The reason for this is that one can no longer combine β and ν_0 dependence simply as ϕ dependence on the right-hand side of (40), because of the implicit dependence of θ on ν_0T_0. This is illustrated schematically in Fig. 4. There is a new line cutting the parabola for each β, with only one of the intersections corresponding to a solution of Eq. (40). What is intriguing is that these are straight lines, in the region of

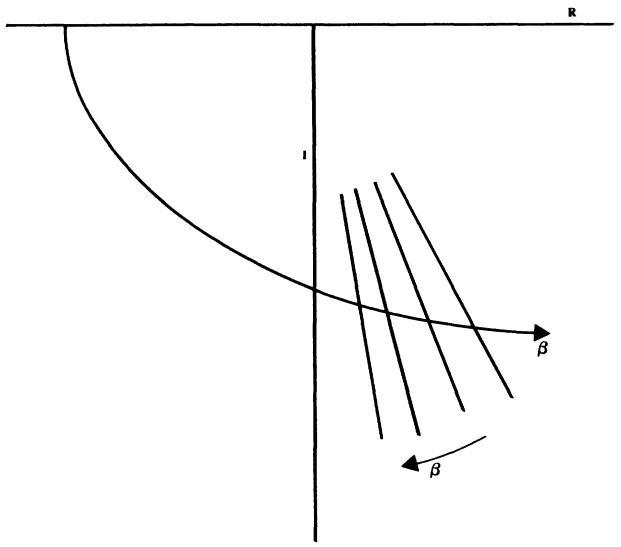

FIG. 4. Here again the parabola is traced out by the real and imaginary parts of the right-hand side of Eq. (38), as β increases. The lines are traced out by the real and imaginary parts of the right-hand side as θ varies, for small θ. There is a different line for each value of β.

interest. Close to the origin, corresponding to large θ, there are loops of a complicated kind, but over the relevant range of θ a straight line is an excellent approximation. In fact, if we equate the ratios of left- and right-hand sides of Eqs. (34) and (35), and work to order θ^4, with $\delta=\frac{1}{2}\gamma\theta^2$, the dependence on θ cancels. The result is an equation for the eigenfrequency β,

$$\beta^2-\Omega_0^2=\frac{\Omega_0}{Q_0T_0}\left[1-\frac{\beta^2T_0^2}{\mu}\right]. \tag{46}$$

Taking account of the relation (45) between the approximate mean delay T_0 and the storage time τ_s, one can see that this result is identical with Eq. (21) for Ω_i. Thus if the eigenfrequency β is identified with the instability frequency Ω_i, our two methods give the same answer.

The characteristic equation can be numerically solved, aided by the graphical method of Fig. 4, without the small θ approximation. Results obtained thus, for the trend with mean delay T and cavity length l, in the case $\gamma=1$, agree with the trends found using the other method. The numerical solutions do not readily reveal as much about the dependence of critical power on all relevant parameters as do the results obtained above, and we have not extended this approach beyond the simple cavity.

CONCLUSION

We have seen that the question of whether cavity interferometers will experience radiation-pressure-induced dynamical instabilities can be addressed in two rather different ways. Both methods, that of studying the characteristic equation and that of finding an effective oscillator equation with frequency dependent terms, give the same results for simple cavity interferometers. The latter method also gives simple results for both broad-band and narrow-band recycled interferometers. The conclusions are clear: while radiation-pressure-induced instabilities may well be important in small interferometers with weak suspensions, they will not be a problem for currently conceived interferometric gravitational wave detectors.

ACKNOWLEDGMENTS

We would like to thank the University of Glasgow and the Science and Engineering Research Council for financial support.

APPENDIX: DESTABILIZATION AND RESTABILIZATION

In this Appendix we examine the characteristic Eq. (39) with $r=\nu_0^{-1}$ and I_0 treated as free parameters, using the stability boundary method.[15–18] (We shall see that the product from rz is more natural here than the ratio r/ν_0.) This characteristic equation is somewhat unusual in having terms of all orders in k. The favored method[19] for equations with a few terms of low k is of no use here, since it works by successively removing terms from the highest k down. However, one can explicitly sum the series on the right-hand side of Eq. (39), which allows us to apply the stability boundary method. We write Eq. (39) as

$$z^2+z\Omega_0/Q_0^2=\Omega_0^2=-gH(rz)\,, \tag{A1}$$

where

$$H(rz)=\Delta^{-1}(e^{rz}+e^{-rz}\cos^2\theta-2\cos\theta\cos\delta)^{-1} \tag{A2}$$

and $g=A\Delta\cos\theta\sin\delta$. When we insert a pure imaginary eigenvalue $z=i\beta$ in Eq. (A1) the left-hand side depends only on β and the right-hand side only on the angle variable $\phi=\beta r$. The stability boundary method begins by seeking intersections of two curves in the complex plane. One is the "ratio curve" $(\beta^2-\Omega_0^2,\ i\beta\Omega_0/Q_0)$, which is traced out as β increases from zero to infinity, and the other is the "delay curve" traced out by the real and imaginary parts of $gH(i\phi)$ as ϕ increases from 0 to 2π. Since the right-hand side of Eq. (40) is now a Fourier series, $H(i\phi)$ is periodic with period 2π. The delay curve is a bounded simple closed curve in the complex plane. The real value $H(0)=1$; the other real value of H is $H(i\pi)$, and it is readily seen that for small θ and δ this value is negative, but very small. The ratio curve starts at $(-\Omega_0^2,0)$, well outside the delay curve, and is unbounded. The two curves either do not intersect, or touch, or intersect twice, as shown in Fig. 2. For very small g the curves do not intersect, and there is stability at all r. If g exceeds a certain critical value, for which the two curves touch, there are two intersections. The pair of critical values β_1,r_1 with r_1 the smaller delay, corresponds to destabilization. We show that the other, with the larger

delay r_2, gives restabilization. In order to determine the stability at a point in r,P space using the stability boundary method, one must proceed in the following way.

(i) Establish stability at a particular point, in fact, one with $r=0$, where the problem is a conventional one, and in this case is trivial. At this point all roots lie in the left-hand half plane.

(ii) Seek solutions β and ϕ of Eq. (A1) for $z=i\beta$, having real positive β and $0<\phi<2\pi$; at these the real part of a pair of conjugate roots changes sign. If there are no such solutions there is stability at all r. The first such solution (meaning that with smallest r) must give a change from stability at low r (all roots have negative real part) to instability at higher r (one pair of roots has positive real part). So at this solution the quantity $d\,\mathrm{Re}z/dr$ is positive.

(iii) For any subsequent solution (larger r, still with $0<\phi<2\pi$) test the sign of this gradient. Denoting

$$z^2+z\Omega_0/Q_0+\Omega_0^2+gH(rz)=P(z)+gH(rz)$$

by $S(r,z)$, this is found, for any simple root, from

$$\frac{dz}{dr}=\frac{-\partial S/\partial r}{\partial S/\partial z}\ . \tag{A3}$$

(The denominator here is zero for a multiple root, at which the ratio curve is tangential to the delay curve.) We introduce the notation $P(z)$ here to emphasize the generality of the method; it does not require any specific form for either $P(z)$ or $H(i\phi)$. If this quantity is negative at the second solution, there is a change back to stability, since the only pair of roots with positive real part now crosses back to the negative half plane.

(iv) We mention this step for completeness although it is not needed in the present application. Repetitions of these intersections for $2n\pi<\phi<2(n+1)\pi$, can give repeated windows of stability, but only for a finite number of repetitions. The successive critical r are

$$r_{1n}=r_1+2n\pi/\beta_1,\quad r_{2n}=r_2+2n\pi/\beta_2\ ,$$

respectively, and in a case such as that considered here the β_1 for instability exceeds the β_2 for stability, so that the two sequences of T values cease to alternate. The argument here is due to Cooke and Grossman.[15] In the present context, however, we are only concerned with small values of ϕ.

In the previous applications of this method the gradient specified in (iii) has been evaluated explicitly for the particular ratio and delay curves used or else, in seeking generality, an alternative method is used which does not employ the ratio curve.[17,19]. Here, because the delay curve is a rather complicated function of ϕ, we give a general argument. The sign of the real part of (A3) is the same as that of the real part of the reciprocal expression

$$\frac{-\partial S}{\partial z}\Big/\frac{\partial S}{\partial r}=\frac{dP}{dz}\Big/\frac{g\partial H}{\partial r}-\frac{\partial H}{\partial z}\Big/\frac{\partial H}{\partial r}$$

$$=\frac{dP}{dz}\Big/\frac{g\partial H}{\partial r}-\frac{r}{z}\ . \tag{A4}$$

Since we only require $z=i\beta$, the second term in (A4) is pure imaginary. Writing

$$P(i\beta)=A(\beta)+iB(\beta)\ ,$$

$$H(i\phi)=U(\phi)+iT(\phi)\ ,$$

the real part of the first term in (A4) is, to within a positive factor,

$$\frac{dA}{dz}\frac{dT}{d\phi}-\frac{dB}{dz}\frac{dU}{d\phi}\ . \tag{A5}$$

At a double root, where $dA/dz=g\,dU/dz$ and $dB/dz=g\,dT/dz$, the quantity (A5) is zero. In fact, the quantity (A5) is the scalar product of two vectors, one pointing tangentially along the ratio curve in the sense of increasing β, and other pointing along the outward normal to the delay curve. At an intersection with the ratio curve crossing the delay curve outwards the sign of $d\,\mathrm{Re}z/dr$ is positive. At an intersection with the ratio curve crossing the delay curve inwards the sign is negative. In the present problem the intersection with higher β and lower ϕ (and so the smaller critical value of r) has $d\,\mathrm{Re}z/dr$ positive, giving destabilization as expected. The intersection with lower β and higher ϕ (and so higher critical r) has $d\mathrm{Re}z/dr$ negative, and gives restabilization.

[1]K. S. Thorne, in *300 Years of Gravitation,* edited by S. W. Hawking and W. Israel (Cambridge University Press, New York, 1987).

[2]V. B. Braginsky and A. B. Manukin, *Measurement of Weak Forces in Physics Experiments* (University of Chicago Press, Chicago, 1977).

[3]A. Dorsel, J. D. McCullen, P. Meystre, E. Vignes, and H. Walther, Phys. Rev. Lett. **51**, 1550 (1983).

[4]P. Meystre, E. M. Wright, J. D. McCullen, and E. Vignes, J. Opt. Soc. Am. B **2**, 1830 (1985).

[5]N. Deruelle and P. Tourrenc, *Gravitation, Geometry and Relativistic Physics* (Springer, Berlin, 1984).

[6]J. M. Aguirregabiria and L. L. Bel, Phys. Rev. A **36**, 3768 (1987).

[7]L. L. Bel, J.-L. Boulanger, and N. Deruelle, Phys. Rev. A **37**, 1563 (1988).

[8]J. M. Aguirregabiria, L. L. Bel, and J.-L. Boulanger, in Proceedings of SOCOS, San José, 1988 (Plenum, New York, in press).

[9]P. Tourrenc and J. M. Aguirregabiria, in Proceedings of IWGWSAP, Amalfi, 1988 (unpublished).

[10]R. W. P. Drever, in *Gravitational Radiation,* edited by N. Deruelle and T. Piran (North-Holland, Amsterdam, 1983).

[11]J.-V. Vinet, B. J. Meers, C. N. Man, and A. Brillet, Phys. Rev. D **38**, 433 (1988).

[12]B. J. Meers, Phys. Rev. D **38**, 2317 (1988).

[13]For example, see M. Born and E. Wolf, *Principles of Optics* (Pergamon, London, 1959).

[14]N. Minorski, J. Appl. Mech. **9**, 65 (1942).

[15]K. L. Cooke and Z. Grossman, J. Math. Anal. Appl. **86**, 592 (1982).

[16]S. P. Blythe, R. M. Nisbet, W. S. C. Gurney, and N. Mac-

Donald, J. Math. Anal. Appl. **109**, 388 (1985).
[17]K. L. Cooke and P. van den Driesche, Funkc. Ekvacioj **29**, 77 (1986).
[18]N. MacDonald, *Biological Delay Systems: Linear Stability Theory* (Cambridge University Press, Cambridge, England, 1989).
[19]K. Walton and J. E. Marshall, Proc. IEED D **134**, 101 (1987).